JOURNAL OF MATERIALS SCIENCE 13 (1978) 173–177

Shrinkage stresses in glass/resin composites

B. HARRIS
School of Materials Science, University of Bath, UK

A simple model has been used to calculate the residual stresses in polyester-resin/glass fibre composites that arise when the material is cooled from the post-curing temperature. An elementary elasticity solution for shrink-fit stresses gives a value of the order of 24 MNm^{-2} for interfacial pressures in a single fibre model, and it appears that this stress is between 10 and 20% lower if the matrix is a hypothetical material having the properties of a composite. The pull-out stress for a glass fibre in polyester resin is estimated to be 7.6 MNm^{-2}, in good agreement with earlier experimental results.

1. Introduction

It has been suggested that in glass-fibre reinforced plastics and carbon-fibre reinforced plastics the work required to pull broken fibres from the matrix after the resin has cracked contributes substantially to the total fracture energy of these composites [1, 2]. It should therefore be possible to estimate the fracture energy if the work required to pull a single fibre from the resin is known. In principle, it should also be possible to estimate this work from a knowledge of the gripping force exerted by the resin on the fibre. Attempts have been made to calculate the stress distributions round fibres resulting from thermal contraction following cooling from the curing temperature [3, 4] and there have also been some experimental studies [5, 6]. In reviewing this work Chamis [7] showed that there is some disagreement between experimental and theoretical results. I have therefore attempted to reassess, on the basis of an extremely simple model, both the magnitude of the frictional bond strength in glass/polyester composites and the extent to which the estimated values agree with experimental results reported by Harris *et al.* [1].

The initial model used is that of an isolated glass fibre in a resin matrix. It is assumed that cure-contraction stresses are relieved during post-curing of the composite at 100° C and that residual stresses develop as a result of cooling from the post-curing temperature ($\Delta T = 80°$ C). The radial interfacial pressure is given by elementary elasticity theory. The properties of constituent materials used in calculation are shown in Table I. The subscripts m and f are used to refer to matrix and fibre, respectively.

TABLE I Properties of glass and polyester resin

Property	Symbol and units	Glass	Resin
Young's modulus	$E(GNm^{-2})$	70	3.5
Poisson's ratio	ν	0.21	0.25
Linear coefficient of thermal expansion	$\alpha(10^{-5}\,°C^{-1})$	1	10

The second stage is to assume that the fibre is embedded in a matrix not of plain resin but of a hypothetical material having the properties of a composite. In this way the effect of matrix properties on interfacial pressure is determined although fibre–fibre interactions are ignored. To do this we assume that the matrix is a pseudo-homogeneous material having the fibre volume fraction V_f and we roughly estimate the properties of the "matrix" by using mixture-rule relationships for expansion coefficient and Poisson's ratio:

$$\alpha'_m = \alpha_f V_f + \alpha_m(1 - V_f)$$

$$\nu'_m = \nu_m V_f + \nu_m(1 - V_f)$$

and a form of iso-stress relationship for Young's modulus:

$$E'_m = \{V_f/E_f + (1 - V_f)/E_m\}^{-1}$$

TABLE II Properties of pseudo-homogeneous matrix

V_f	E' (GNm^{-2})	α'_m ($10^{-5}\,°C^{-1}$)	ν'_m
0	3.50	10	0.250
20	4.32	8.2	0.242
30	4.90	7.3	0.238
40	5.65	6.4	0.234
50	6.67	5.5	0.230
60	8.14	4.6	0.226
70	10.45	3.7	0.222

The primed symbols indicate that they refer to a "modified" matrix. Table II shows the properties of the modified matrix as a function of filler content calculated in this way.

2. Fibres in a resin matrix

A rough estimate of the lateral interfacial pressure when a single, infinitely-rigid fibre is embedded in resin is given by

$$p \approx E_m \Delta T \Delta\alpha$$

or $25.2\,MNm^{-2}$, but for a glass fibre the real pressure will be lower than this. The lateral pressure developed when the resin contracts laterally onto the fibre during cooling can be obtained by the elementary elasticity approach used for calculating shrink-fits [8] which gives the pressure, p, referring to Fig. 1, from the expression

$$\frac{\delta/c}{\frac{1}{E_m(1-c^2/b^2)}\{(1-\nu_m)c^2/b^2 + (1+\nu_m)\} + \frac{(1-\nu_f)}{E_f}} \quad (1)$$

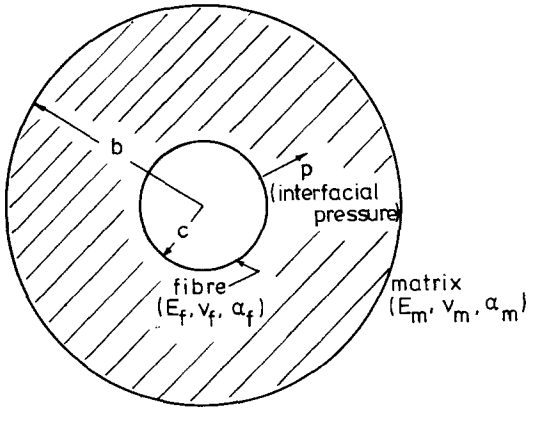

Figure 1 Schematic illustration of geometric and physical parameters involved in calculating the shrinkage stress in a fibre/resin composite. The radial stress σ_{rr}, is equal to p at the interface and falls off with distance into the resin.

In this equation δ is the difference between the radial displacements of the fibre and matrix surfaces at the interface radius, c, i.e. the amount by which the room-temperature radius of the fibre exceeds the bore radius of the hole that would have been left in the resin had the fibre not been present. δ is calculated in the following way. Let r_f be the radius of the fibre at room-temperature and r_m be the radius at room temperature of the resin hole that was created at 100° C by a fibre of radius $r_f\,(1 + \alpha_f \Delta T)$. For a notional 0.3 mm diameter fibre (see Reference 1 for example) r_f is thus 0.15 mm, the fibre radius at post-curing temperature is 0.15012 mm, and the resin hole radius (with the fibre *not* present) after cooling from the curing temperature would be

$$r_m = \frac{0.15012}{1 + \alpha_m \Delta T} = 0.14893\,\text{mm}.$$

Hence the relative displacement, δ, which is $(r_f - r_m)$. The effective shrink-fit strain in the numerator of Equation 1 is obtained by dividing δ by the equilibrium radius, c, of resin hole and fibre at 100° C ($c = 0.15012$ mm). b in Equation 1 is simply the outer diameter of the resin cylinder. From Equation 1 we obtain p as a function of the ratio c/b for a single fibre embedded in resin, as shown in Fig. 2. The limiting thickness of a resin block that will grip the fibre with maximum force is thus about twenty times the fibre diameter. By making the assumption now that the matrix has the properties of a composite, as given in Table II, we can determine new values for δ and so obtain the interfacial pressure as a function of fibre

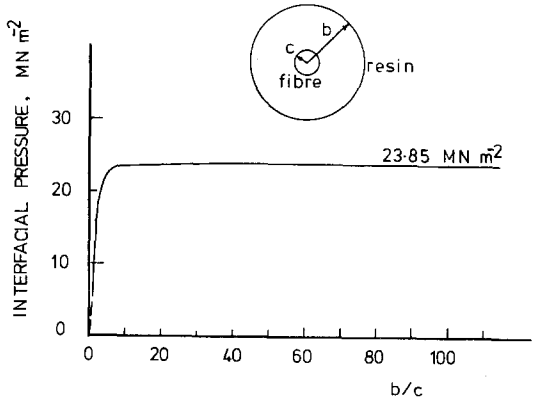

Figure 2 The interfacial pressure as a function of the relative diameters of the matrix and fibre. The curve is the solution to Equation 1 and takes into account the fact that the fibre is compressed along its axis as well as laterally.

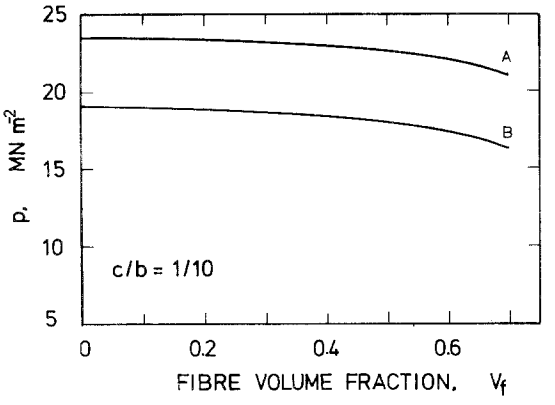

Figure 3 Interfacial pressure as a function of fibre volume fraction, assuming that the matrix is a pseudo-homogeneous material with the properties of a composite with volume fraction V_f. In curve A the longitudinal shrinkage constraint is included in the calculation: in curve B the effect of this constraint is omitted.

volume fraction for our artificial composite. The results, given in Fig. 3, show that p falls only slowly with V_f from the single fibre value of 19.05 MNm^{-2} (for $c/b = 0.1$) to 17.37 MNm^{-2} for a typical 70% glass fibre composite. For comparison the pressure exerted by the same resin on a single glass sphere can easily be shown to be 38.5 MNm^{-2}, and in a particulate composite with $V_f = 0.50$ this falls to 35.8 MNm^{-2}.

Shrink-fit models used by engineers usually ignore longitudinal constraints and assume that the inner shaft and outer cylinder will slide over each other during cooling from the fitting temperature. In a composite the resin will adhere strongly to the glass at the post-curing temperature and will exert a strong axial compression when the composite is cold. Treating the lateral and longitudinal constraints as separate and additive, we see that a single fibre will experience an axial compressive strain of about 0.008, equivalent to a stress in the fibre of 556 MNm^{-2}. This is nearly half its tensile breaking stress and is clearly sufficient to cause elastic buckling of the kind observed by Dow [9] and Arrington [10] if the resin is sufficiently flexible. This axial stress causes a radial expansion of the fibre of about 0.17% and the strain function δ/c in Equation 1 is increased by a factor ranging from 1.23 for the single fibre case to 1.29 for a 70% fibre composite. The interfacial pressure for the single fibre model with axial constraint is therefore 23.5 MNm^{-2} (for $c/b = 0.1$) and the variation with fibre content is as shown in Fig. 3. From these results, therefore, we see that the calculated values of interfacial pressure are not likely to be strongly sensitive to matrix properties because of the inter-relationship between elastic modulus, Poisson's ratio, and expansion coefficient. For the same reason they are not greatly affected by the crudeness of the relationships used to estimate E'_m, ν'_m and α'_m. This insensitivity to materials properties (other than the large matrix shrinkage) is also reflected in estimated values of p for carbon-fibre/resin systems. If we take a zero expansion coefficient for carbon fibres and estimate p for a single fibre in polyester resin, ignoring the axial constraint, we obtain values of 21.65 and 21.54 MNm^{-2} for types I and II carbon fibre whose moduli are roughly 400 and 200 GNm^{-2}, respectively. For a composite with 50% of type I carbon fibres this figure is reduced only slightly to 21.18 MNm^{-2}. For boron fibres, with a modulus of about 400 GNm^{-2} and an expansion coefficient of 1.6×10^{-6}, we expect similar values. These are only 10% or so higher than the figure for glass/polyester.

3. Discussion and conclusions

The values of interfacial pressure calculated here are substantially greater than those usually quoted. Daniel and Durelli [5] for example, report measured values of 4.9 MNm^{-2}. Haener *et al.* [3] used classical elasticity methods to investigate microresidual stresses round fibres for a model with $V_f = 0.64$ in which the matrix was assumed to shrink by 1% on cooling while the fibres did not shrink at all. They found that the radial pressure acting on one fibre varies with position relative to the other nearby fibres. For a composite with hexagonal symmetry (Fig. 4) and a modulus ratio,

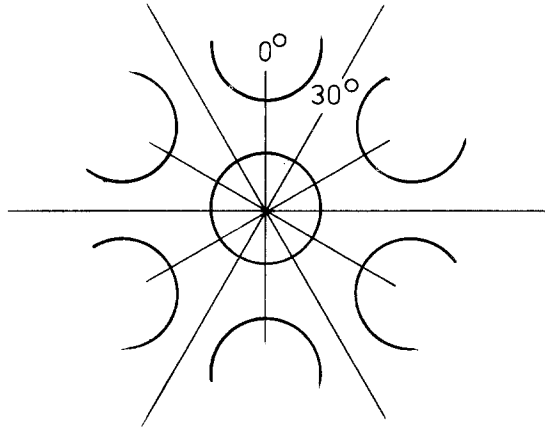

Figure 4 Hexagonal symmetry of composite model used in the calculations of Haener *et al.* [3] and Chamis [4].

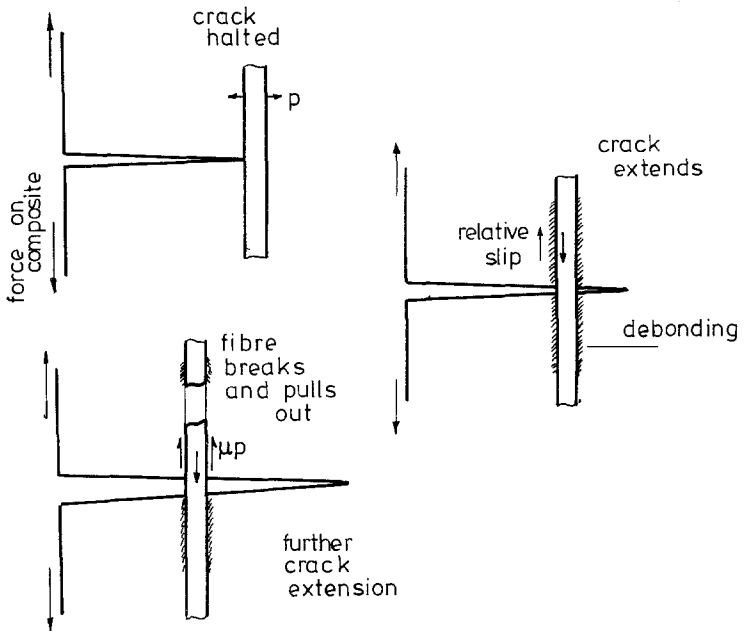

Figure 5 Steps in the propagation of a crack past a fibre.

E_f/E_m, of about 26, their results indicate that the compressive radial stress is about 17.5 MNm^{-2} along close-packed directions (0°) but that it falls to zero at about 20° and, changing sign, becomes a tensile stress of about 5 MNm^{-2} at 30°. Similar results have also been reported by Owen [11]. Variations of this kind in interfacial pressure would seem to imply that good bonding can never be achieved in high modulus fibre composites, for with such a stress distribution there must always be either a real or an incipient debond. It seems unlikely that this could be so, however, in view of all the available visual evidence of failure surfaces in composites.

When composites are loaded so that fibres break inside the resin away from a major resin crack, large quantities of work may be required to pull the broken fibre ends out of the matrix. This work is done in overcoming the frictional drag resulting from the shrinkage grip of resin on fibre. The sequence of events prior to pull-out may be something along the following lines (Fig. 5):

(i) A major resin crack moves through the composite. Its progress is hindered by fibres which, with their higher elastic rigidity, prevent the crack-opening displacement (cod) from reaching a critical level.

(ii) Relative shear between fibre and resin aids debonding and the cod increases, allowing further extension of the resin crack. Debonding is a process which may or may not involve breaking of chemical bonds, but which certainly releases the locked-in longitudinal shrinkage constraint discussed earlier. Some work is done when the relative shear displacement occurs because the lateral shrinkage pressure is still present.

(iii) The fibre breaks within the debonded region and is subsequently pulled out of the resin against the frictional shrinkage grip.

For the case of model double cantilever beam samples used by Harris *et al.* [1] we may assume $V_f \to 0$. In loading up these samples, then, first signs of debonding should occur when the fibre stress is μp. We do not know the exact value of the friction coefficient, μ, for a fresh glass surface against a fresh, cast resin counterface, but if we take the value of 0.4 quoted in handbooks for hard glassy polymers and thermoset resins of the epoxide and polyester types, we obtain $\mu p = 9.4\,MNm^{-2}$. After fibre failure the work required to overcome the frictional grip with axial constraint relaxed will be about 20% lower than this, or 7.6 MNm^{-2}. This value is in good agreement with the measured values of 6 MNm^{-2} and 8.6 MNm^{-2} quoted by Harris *et al.* for clean fibres and silane coated fibres, respectively. These values refer however to the initial friction stress operating at the onset of pull-out, and the experimental evidence in their paper suggests that interface conditions may change drastically during the pull-out process. The value for p reported by Daniel and Durelli and the calculated values of Haener *et al.*

(averaged out over all orientations) would not give satisfactory agreement with experimental friction stress results.

In conclusion, since the release of axial shrinkage stress results in a substantial reduction of the frictional force between fibre and matrix, the debonding process may be an even smaller contributor to total fracture energy than is often supposed [12]. And an inference from the model of crack propagation proposed above is that the Cook and Gordon mechanism of crack inhibition [13], originally postulated for laminated structures, could not work in polyester/glass fibre composites because axial cracking (debonding) is essential if crack extension is to occur.

References

1. B. HARRIS, J. MORLEY and D. C. PHILLIPS, *J. Mater. Sci.* **10** (1975) 2050.
2. B. HARRIS, P. W. R. BEAUMONT and E. M. DE FERRAN, *ibid.* **6** (1971) 238.
3. J. HAENER, N. ASHBOUGH, C. Y. CHIA and M. Y. FENG, "Investigation of Micromechanical Behaviour of Fibre Reinforced Plastics 1968," Technical report USAAV LABS-TR-67-66 (AD-667901).
4. C. C. CHAMIS, Mechanics of Load Transfer at Fibre–Matrix Interface, 1972, NASA Report TN D-5367.
5. I. M. DANIEL and A. J. DURELLI, 16th Annual Technical Conference of SPI, Paper 19-A, 1961.
6. P. S. THEOCARIS and E. MARKETOS, *Fibre Science and Technology* **3** (1970) p. 21.
7. C. C. CHAMIS, "Composite Materials," edited by L. J. Broutman and R. H. Krock, Vol. 6 (Academic Press, London, 1976).
8. D. S. DUGDALE, "Elements of Elasticity", (Pergamon, Oxford, 1968) p. 95.
9. N. F. DOW, B. W. ROSEN and Z. HASIN, Studies of Mechanics of Filament Composites, 1966, NASA report C R-492.
10. M. ARRINGTON, D. Phil. Thesis, University of Sussex, 1976.
11. M. J. OWEN, "Composite Materials", edited by L. J. Broutman and R. H. Krock, Vol. 5, (Academic Press, London, 1974) p. 313.
12. M. C. MURPHY and J. O. OUTWATER, 28th Annual Technical Conference, Reinforced Plastics/Composites Institute of SPI, Paper 17-A, 1973.
13. J. COOKE and J. E. GORDON, *Proc. Soc.* **A282** (1964) 508.

Received 18 April and accepted 8 June 1977.